Title

Evolutionary and functional analyses reveal a role for the RHIM in tuning RIPK3 activity across vertebrates

Authors

Elizabeth J. Fay[1], Kolya Isterabadi[1], Charles M. Rezanka[1], Jessica Le[1], Matthew D. Daugherty[1]*

Affiliations

[1]Department of Molecular Biology, School of Biological Sciences, University of California, San Diego, La Jolla, CA, 92093

* To whom correspondence should be addressed: Matthew D. Daugherty (mddaugherty@ucsd.edu)

Abstract

Receptor interacting protein kinases (RIPK) RIPK1 and RIPK3 play important roles in diverse innate immune pathways. Despite this, some RIPK1/3-associated proteins are absent in specific vertebrate lineages, suggesting that some RIPK1/3 functions are conserved while others are more evolutionarily labile. Here, we perform comparative evolutionary analyses of RIPK1-5 and associated proteins in vertebrates to identify lineage-specific rapid evolution of RIPK3 and RIPK1 and recurrent loss of RIPK3-associated proteins. Despite this, diverse vertebrate RIPK3 proteins are able to activate NF-κB and cell death in human cells. Additional analyses revealed a striking conservation of the RIP homotypic interaction motif (RHIM) in RIPK3, as well as other human RHIM-containing proteins. Interestingly, diversity in the RIPK3 RHIM can tune activation of NF-κB while retaining the ability to activate cell death. Altogether, these data suggest that NF-κB activation is a core, conserved function of RIPK3, and the RHIM can tailor RIPK3 function to specific needs within and between species.

32

33 **Introduction**

34 Receptor interacting protein kinase 3 (RIPK3), and the closely related kinase
35 RIPK1, have critical roles in mediating cell death and inflammatory signaling [1].
36 Downstream of signals from innate immune receptors like Z-DNA binding protein 1
37 (ZBP1) and tumor necrosis factor receptor 1 (TNFR1), RIPK3 and RIPK1 interact via their
38 shared RIP homotypic interaction motif (RHIM) to form amyloid-like aggregates [2],
39 leading to their autophosphorylation and activation of additional effector proteins to carry
40 out their innate immune functions. For example, RIPK3 can phosphorylate MLKL to
41 activate highly inflammatory programmed necrotic cell death (necroptosis) [3], RIPK1/3
42 can engage caspase-8 (CASP8) to activate apoptotic caspases [4, 5], or RIPK1/3 can
43 activate the pro-survival and pro-inflammatory transcription factor NF-κB [6, 7]. Several
44 factors are known to impact the outcome of RIPK1/3 activation, such as the activating
45 signal and caspase activity [1, 8]. Altogether, RIPK3 and RIPK1 are central to determining
46 cell fate downstream of various innate immune stimuli.

47 Like many innate immune proteins, RIPK3 is evolutionarily dynamic in vertebrates.
48 Phylogenomic analyses of a small number of species from different vertebrate clades
49 suggest that RIPK3, and the associated proteins ZBP1 and MLKL, have been lost in some
50 vertebrate lineages including birds, carnivores, and marsupials [9, 10]. In addition, RIPK3,
51 RIPK1, MLKL, and ZBP1 are known to interact with viral proteins [11-16] and have been
52 shown to be evolving under recurrent positive selection in both primates and bats [17,
53 18], a hallmark of host proteins that directly interact with viral proteins [19]. Despite the
54 known evolutionary divergence of RIPK3 in vertebrates, most of what is known about their
55 activation and regulation is from studies conducted in humans and mice. Even between
56 humans and mice, there are known differences in the roles of specific genes in regulation
57 of NF-κB, suggesting this pathway can be tailored to the distinct environments of different
58 species [20]. These differences likely extend beyond humans and mice, and likely include
59 RIPK1/RIPK3 mediated activation of NF-κB. Furthermore, RIPK1 and RIPK3 are part of
60 a larger family of RIPKs, including RIPK2, RIPK4, and ANKK1/RIPK5, which, with the
61 exception of RIPK5, are known to activate NF-κB in various cellular contexts [21-23]. The

62 degree to which these other RIP kinases and their interacting partners have diversified
63 across vertebrates is unknown.

64 Here, we use evolutionary and functional approaches to characterize
65 diversification of RIPK3-mediated activation of NF-κB. We identified RIPK1- and RHIM-
66 mediated activation of NF-κB by diverse vertebrate RIPK3 proteins, as well as distinct
67 mechanisms of RIPK3-mediated activation of NF-κB. Phylogenetic and phylogenomic
68 analyses of RIPK1-5 and several key associated proteins revealed the dynamic evolution
69 of RIPK3 and RIPK1. In addition to observing the loss of RIPK3 and necroptosis-
70 associated proteins in some vertebrate lineages, we identify changes in regulatory
71 features—including catalytic sites and CASP cleavage sites—in RIPK3 and RIPK1 in
72 specific mammalian lineages that may affect their function. Intriguingly, we found that the
73 RHIM domain of RIPK3 and RIPK1, as well as other RHIM-containing proteins, is highly
74 conserved in vertebrates and in a non-vertebrate RIPK1 protein. Consistent with this
75 strong conservation of the RHIM domain, we found that RIPK1 proteins from diverse
76 vertebrates, and even a non-vertebrate RIPK1, are able to activate NF-κB, suggesting
77 that activation of this inflammatory response is a conserved function of RIPK3, RIPK1,
78 and potentially other RHIM-containing proteins in vertebrates. Altogether, these data
79 suggest that activation of NF-κB is the ancestral and conserved feature of RIPK3 and
80 RIPK1, while other functions such as necroptosis are more evolutionarily labile and
81 rapidly evolving, likely as a response to evolutionary pressure from pathogens.

82

83 **Results**

84 *Comparative evolutionary analysis of RIPK1-5*

85 To understand the evolution and diversification of RIPK function, we first wished to
86 compare the functions of human RIPKs. There are canonically four RIPKs in humans,
87 RIPK1-4. ANKK1 is a close paralog of RIPK4 and has therefore been denoted as RIPK5.
88 Additional proteins have also been described as RIPK proteins, including DSTYK,
89 LRRK1, and LRRK2, but these proteins are phylogenetically distinct and will therefore not
90 be considered here [23]. The shared domain architecture of RIPK1-5 includes a
91 conserved N-terminal kinase domain, an extended disordered intermediate domain, and
92 distinct protein interaction domains at the C-terminus that can include a death domain

93 (DD), RIP homotypic interaction motif (RHIM), caspase activation and recruitment domain
94 (CARD), or ankyrin repeats (ANK) (Figure 1A). Human RIPK1-4 activate NF-κB, albeit
95 through different mechanisms, including differential dependence on endogenous RIPK1
96 and kinase activity (Supplementary Figure 1-3). Interestingly, despite its close homology
97 to RIPK4, RIPK5 did not activate NF-κB. Altogether, these data highlight NF-κB as a
98 shared function of RIPK1-4.

99 We next wished to perform comparative evolutionary analyses of RIPK1-5 in
100 vertebrates to determine which RIPKs might be undergoing functional divergence. We
101 first analyzed RIPK1-5 in four distinct mammalian clades to determine whether there was
102 evidence of recurrent positive selection, which can be a hallmark of host-pathogen
103 interactions and can drive functional diversification. Notably, we only found evidence for
104 positive selection acting on RIPK1 and RIPK3 (Fig 1B, Supplementary files 1-2).
105 Interestingly, RIPK1 and RIPK3 are not uniformly evolving under positive selection in all
106 mammalian clades analyzed. For instance, in primates, RIPK3 is evolving under strong
107 positive selection, where RIPK1 is not, consistent with previous data [17, 18]. In contrast,
108 ungulate RIPK3 does not show evidence for positive selection whereas ungulate RIPK1
109 does. These data indicate that among RIPK1-5, only RIPK1 and RIPK3 genes have
110 undergone recurrent positive selection, and that RIPK1 and RIPK3 may have faced
111 different selective pressures across distinct mammalian lineages.

112 In addition to evolving under positive selection in primates and bats [17], RIPK3,
113 ZBP1, and MLKL are known to be lost in some vertebrate lineages [9]. However, it is
114 unknown if other RIPK and RIPK-associated proteins are similarly lost. We therefore
115 performed phylogenomic analysis on 489 vertebrate species for the presence or absence
116 of RIPK1-5 and several key RIPK-associated proteins (Figure 1C, Supplementary Files 4
117 and 5). Due to the difficulty in discerning whether a gene absence in an individual species
118 is due to true gene loss or incomplete genome assembly, we focused on multi-species
119 patterns of gene loss within and between vertebrate lineages. Given that NF-κB is broadly
120 present in many vertebrate and non-vertebrate species, including horseshoe crab [24],
121 *Drosophila melanogaster* [25], and cnidarians and bivalves (reviewed in [26]), we
122 analyzed proteins associated with other RIPK functions. We first confirmed the loss of
123 necroptosis associated proteins that has been previously reported [9]: RIPK3 and ZBP1

124 in birds; RIPK3, ZBP1, and MLKL in marsupials; MLKL in carnivores. In addition, we found
125 that ZBP1 is absent in all fish species, suggesting that this protein, and ZBP1-mediated
126 necroptosis, arose only during tetrapod evolution.

127 We then analyzed RIPK1 and its associated proteins. RIPK1 is found nearly every
128 vertebrate genome queried, as well as clear homologs in several non-vertebrate species,
129 including zebra mussel (*Dreissena polymorpha*), several additional spiralia species, and
130 lancelet species in the genus *Branchiostoma* (accession numbers in Supplementary File
131 4). Homologs—defined as proteins with a homologous N-terminal kinase domain and a
132 C-terminal RHIM tetrad and death domain—were not found in tunicates, echinoderms,
133 cnidarians, nematodes, arthropods, or amoeba. Additional RIPK-like proteins have been
134 found in other non-vertebrate species, including a RIPK1/2-like protein in *Drosophila* and
135 other protostomes [9], although these proteins were not considered here due to minimal
136 sequence similarity to the human RIP kinase domains and our focus on vertebrate RIP
137 kinases. We also identified caspase-8 (CASP8), a known regulator of RIPK1, and its
138 closest homolog, CASP10. Due to the similar domain structure of CASP8 and CASP10,
139 we only identified whether a species has a single CASP8/10 protein, two distinct
140 CASP8/10 proteins as determined by phylogeny (see Materials and Methods), or none.
141 At least one copy of CASP8/10 is found in most tetrapod genomes, although it is absent
142 sea lamprey. Two copies, presumably marking the delineation between CASP8 and
143 CASP10, began in tetrapod, coinciding with the emergence of ZBP1. This may reflect the
144 role of CASP8 in regulating ZBP1, and duplication of this caspase allowed for the
145 specialized function of CASP8 [27]. We also confirmed the loss of CASP10 in some
146 rodents [28] (see Supplementary Figure 4A for CASP8/10 breakdown), revealing that
147 suborder Myomorpha ("mouse-like") and Castorimorpha ("beaver-like") rodents have lost
148 CASP10, whereas Sciuromorpha ("squirrel-like") and Hystricomorpha ("porcupine-like")
149 rodents have retained CASP10. Finally, we found that FADD and TRIF are well conserved
150 in all vertebrates.

151 We also analyzed the phylogenomic distribution of RIPK2, 4, and 5 and their
152 associated proteins. RIPK2 and its associated protein NOD1 are found in most
153 vertebrates [21, 22]. Intriguingly, we observed a second paralog of RIPK2, which we call
154 RIPK2B, in many vertebrates but lost in therian (live-bearing) mammals (Supplementary

155 Figure 4B). NOD2 is present in lamprey and fish, but absent in birds, reptiles, and some
156 amphibians, including some of the same species that contain RIPK2B. While RIPK2B
157 retains both the kinase domain and CARD, there may be distinct regulatory mechanisms,
158 specifically those related to NOD2, compared to RIPK2. RIPK4 is present in jawed
159 vertebrates. IRF6, the only known phosphorylation target of RIPK4 [21, 22], emerged prior
160 to RIPK4 and has been lost in many vertebrate species, particularly in carnivores,
161 cetaceans, and ungulates. RIPK5, which has no known function and no known interacting
162 proteins, has been lost in several lineages, including monotremes and lagomorphs.
163 Overall, our analyses revealed that RIPK1 and RIPK3 are evolutionarily distinct from other
164 RIP kinases, and the recurrent loss of some RIPK1/3-associated necroptosis proteins
165 (ZBP1, MLKL, CASP8) and RIPK3 suggests that these proteins may have functions
166 tailored to the needs of specific vertebrate lineages.

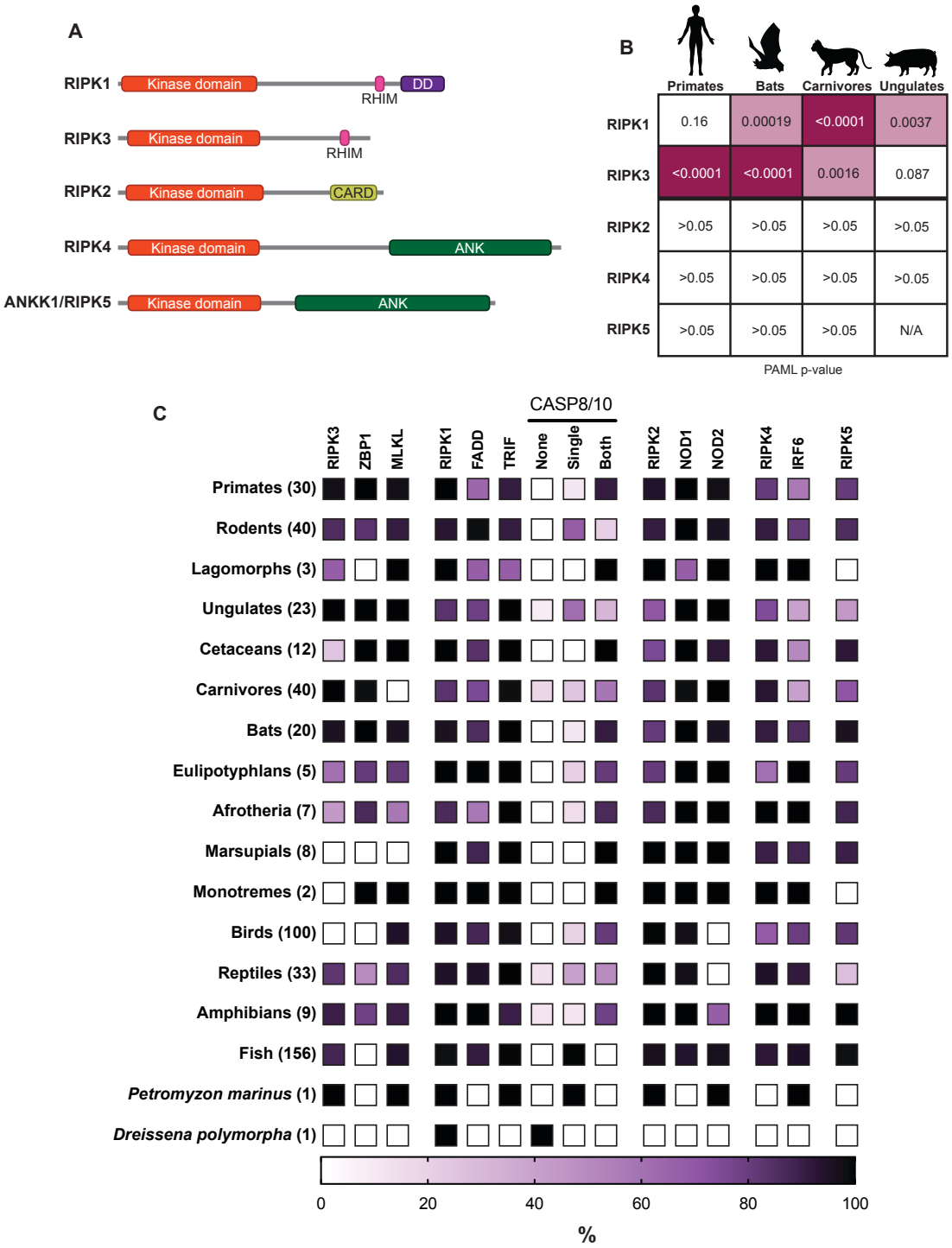

Figure 1. Comparative evolutionary analysis of RIPK1-5. (A) Domain structures of human RIP kinases. RHIM = RIP homotypic interaction motif, DD = death domain, CARD = caspase activation and recruitment domain, ANK = ankyrin repeats. (B) Positive selection analysis of RIPK1-5 in the indicated mammalian order. Input sequences and PAML p-values can be found in Supplementary Files 1 and 2. Images of model species generated using BioRender. (C) Heat map showing the percentage of species within a clade that have the indicated protein. The clades and the number of species within each clade are indicated on the left. Complete lists of proteins and species in each

group can be found in Supplementary Files 4 and 5. Lancelet species were not queried for all proteins and are not included in this graph.

Diverse vertebrate RIPK3 proteins activate NF-κB

Our analyses revealed dynamic evolution of RIPK3 in vertebrates, including signatures of positive selection in multiple mammalian clades and recurrent loss of RIPK3 and its associated proteins. We hypothesized that this rapid RIPK3 evolution may have resulted in different functions of RIPK3 in different vertebrate lineages. We therefore tested the ability of RIPK3 proteins from diverse vertebrates, ranging from 23-63% similarity to humans (Fig 2A, Supplementary Figure 5), to activate NF-κB in human cells. We included two mammalian species that retain all necroptosis proteins (mouse, *Mus musculus*; pig, *Sus scrofa*), a mammalian species lacking a necroptosis protein (cat, *Felis catus*), reptilian species that do (turtle, *Chelonia mydas*) and do not (lizard, *Anolis carolinensis*) retain all necroptosis proteins, and sea lamprey (*Petromyzon marinus*) as our most distal vertebrates relative to humans. To our surprise, among all vertebrates tested, only pig and sea lamprey RIPK3 failed to activate NF-κB in human cells (Fig 2B). This striking conservation of function indicates that NF-κB activation has remained intact despite lineage specific RIPK3 divergence and loss of interacting partners. We then analyzed whether, like human RIPK3 (Supplementary Figure 1C) [29], other vertebrate RIPK3 proteins require RIPK1 to activate NF-κB by repeating experiments in RIPK1 KO cells. Interestingly, while mammalian RIPK3 activation is dependent on RIPK1, both lizard and turtle RIPK3 activate NF-κB independently of RIPK1 (Fig 2B). These results indicate that the requirements for NF-κB activation by RIPK3 are species-specific.

Finally, we tested whether another function of RIPK3, activation of ZBP1- and MLKL-dependent cell death (Supplementary Figure 6), is also conserved. Most mammalian RIPK3 proteins were able to activate cell death using human ZBP1 and MLKL (Fig 2C). This included pig RIPK3, which is unable to activate NF-κB, suggesting that activation of cell death and NF-κB by RIPK3 proteins have been separated in a species-specific manner. Likewise, we observed that cat RIPK3 can activate NF-κB but fails to activate cell death. Based on this observation, we analyzed the sequences of carnivore RIPK3 proteins and found that feline RIPK3 have mutated kinase catalytic residue (Supplementary Figure 7), explaining the loss of cell death activation by cat RIPK3.

207 Outside of mammals, only lizard RIPK3 was able to activate cell death, despite the ability
208 of both lizard and turtle RIPK3 to activate NF-κB, further suggesting that these functions
209 of RIPK3 have distinct, species-specific requirements.

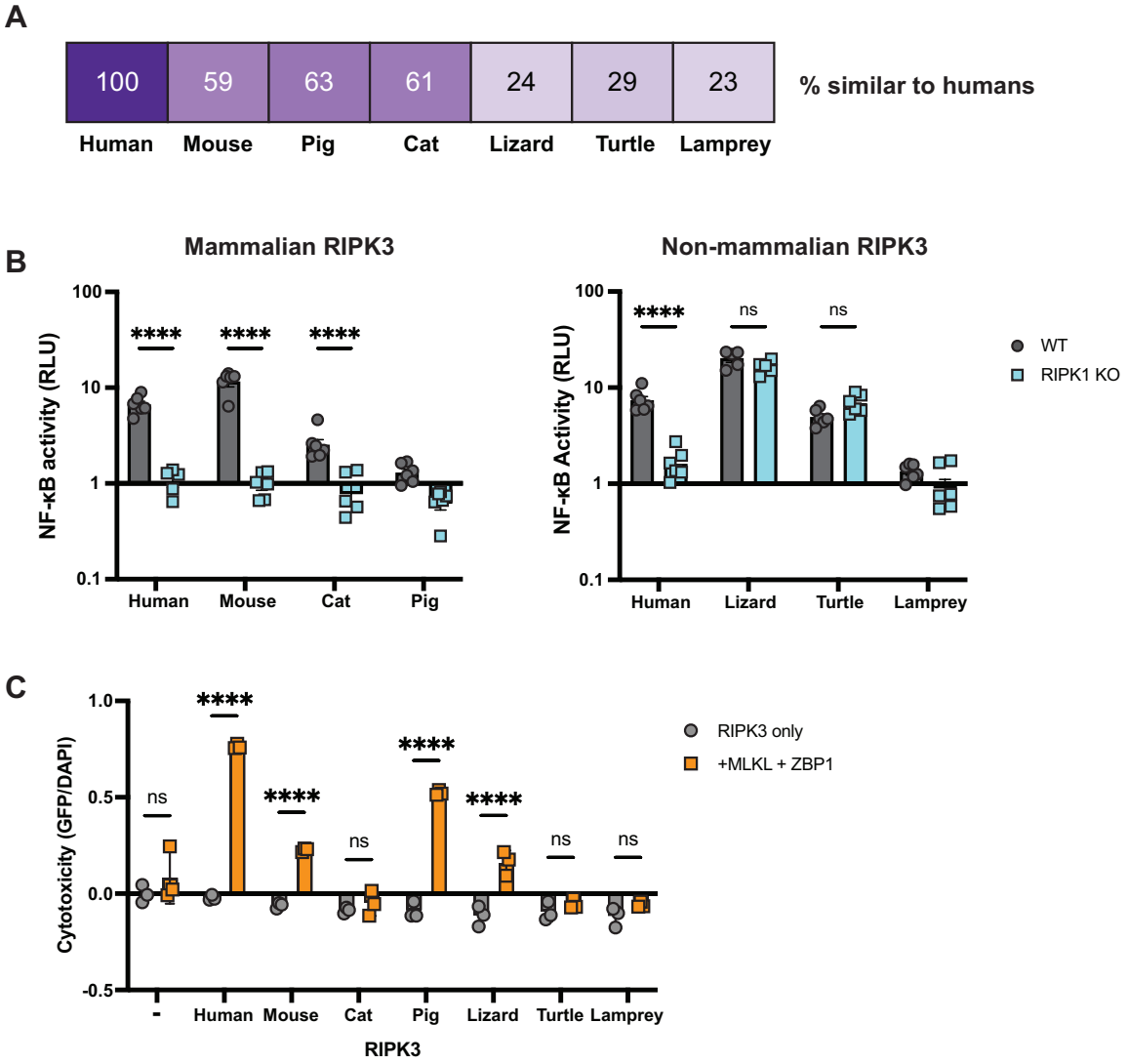

210

211 **Figure 2.** Diverse vertebrate RIPK3 proteins activate NF-κB. (A) Percent similarity of RIPK3 from
212 the indicated species compared to humans. (B) RIPK3 proteins were transfected into WT or RIPK1
213 KO HEK293T cells, along with NF-κB firefly luciferase and control renilla luciferase reporter
214 plasmids (see Materials and Methods), and NF-κB activity was measured at 18h post-transfection.
215 (C) RIPK3 proteins were transfected into HEK293T cells with and without human ZBP1 and MLKL.
216 At 18h post-transfection, cells were stained using the ReadyProbe Cell Viability kit and
217 fluorescence was measured using a plate reader. Species shown are mouse (*Mus musculus*), cat
218 (*Felis catus*), pig (*Sus scrofa*), lizard (*Anolis carolinensis*), turtle (*Chelonia mydas*), and lamprey
219 (*Petromyzon marinus*). Data are representative of 3-5 independent experiments with n=3-6
220 replicates per group. Data were analyzed using two-way ANOVA with Šidák's multiple comparisons
221 test. ns = not significant, **** = p<0.0001.
222

223 *Conservation of the RHIM sequence determines RIPK3 activation of NF-κB*

224 The conservation of NF-κB activation by RIPK3 proteins that share as little as 24%
225 sequence identity and are up to >300 million years diverged [30] suggests some regions
226 of the protein are likely highly conserved. To identify such regions, we returned to our
227 positive selection analyses. While we identified rapidly evolving sites throughout the
228 primate RIPK3, there was a cluster of sites in and around the C-terminal RHIM (Fig 3A
229 Supplementary File 5), which is a known region of interaction between RIPK1 and RIPK3
230 and RIPK3 homooligomerization [2, 31]. Intriguingly, despite multiple rapidly evolving
231 sites within the RHIM, a core tetrad (VQVG) is not rapidly evolving. Similarly, the core
232 tetrads of bat and carnivore RIPK3 are not rapidly evolving (Fig 3B). Furthermore, the
233 RIPK3 core RHIM tetrad is highly conserved across vertebrates (Fig 3C). This is despite
234 loss of other functional motifs in specific lineages, including loss of the RIPK3 catalytic
235 site in felines (Supplementary Figure 7).
236 We therefore tested whether this conserved RHIM tetrad was responsible for
237 activation of NF-kB by diverse vertebrate RIPK3s. We mutated the RIPK3 RHIM core
238 tetrad (V/I-Q-V/I-G to AAAA) in our panel of vertebrate RIPK3 proteins and tested the
239 ability of these proteins to activate NF-kB in human cells. Mutation of human, mouse, and
240 cat RIPK3 RHIMs reduced activation of NF-κB as expected (Fig 3D, Supplementary
241 Figure 5). Surprisingly, despite activating independently of RIPK1 (Fig 2B), activation of
242 NF-κB by lizard and turtle RIPK3 remains dependent on the RHIM (Fig 3E, left), and
243 independent of RIPK3 kinase activity (Supplementary Figure 8-9). These data support
244 that reptile RIPK3 activates NF-κB through a distinct mechanism from mammalian RIPK3,
245 but one that is still highly dependent on the RHIM core tetrad. Interestingly, while
246 analyzing RHIM domains of non-human RIPK3, we observed that the sea lamprey RHIM
247 diverges from the canonical V/I-Q-V/I-G tetrad and instead contains TQIG (Fig 3C). To
248 determine if this was responsible for the limited activation of NF-κB by sea lamprey
249 RIPK3, we mutated this motif to IQIG and observed an increase in NF-κB activation (Fig
250 3E, right). Altogether, these data indicate that NF-κB activation is a conserved function of
251 RIPK3 that requires conservation of the core RHIM tetrad, but allows for substantial
252 sequence divergence elsewhere in the protein.

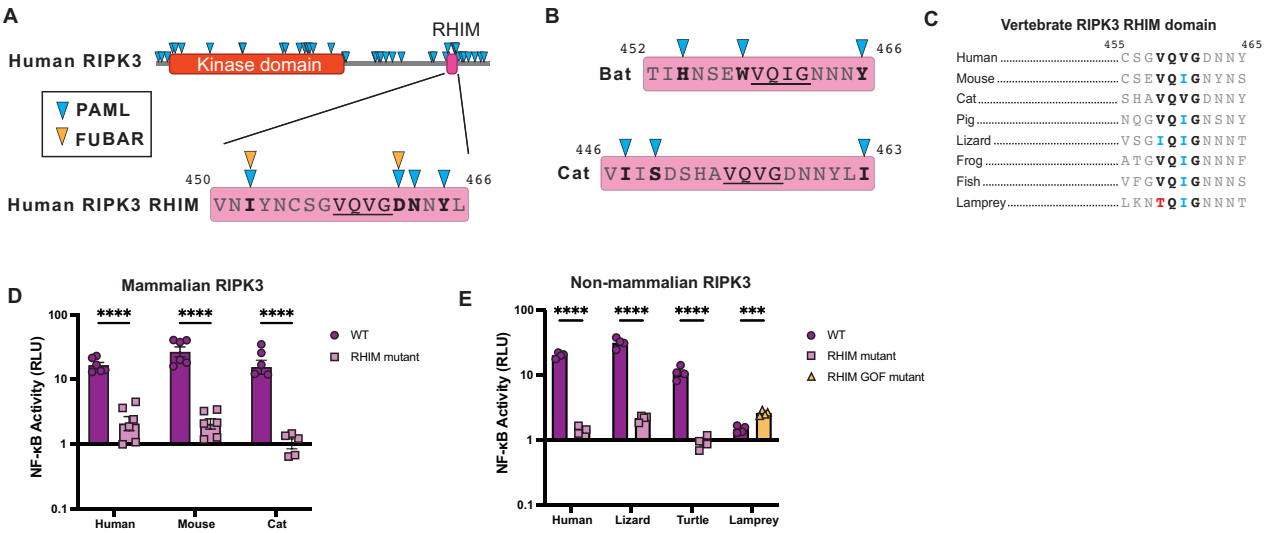

Figure 3. Conservation of the RHIM sequence determines RIPK3 NF-κB activation. A) Residues evolving under positive selection as identified using PAML and FUBAR (see Materials and Methods) in primate RIPK3 and the primate RIPK3 RHIM domain mapped on the human sequence. (B) Residues evolving under positive selection in bat and carnivore RIPK3, mapped on to the *Sturnira hondurensis* and *Felis catus* sequences respectively. (C) Alignments of the RIPK3 RHIM across diverse vertebrates. Residue numbers refer to the human sequence. (D-E) Mammalian (D) and non-mammalian (E) RIPK3 proteins were transfected into WT HEK293T cells along with NF-κB firefly luciferase and control renilla luciferase reporter plasmids (see Materials and Methods). NF-κB activity was measured at 18h post-transfection. Species shown are mouse (*Mus musculus*), cat (*Felis catus*), pig (*Sus scrofa*), lizard (*Anolis carolinensis*), turtle (*Chelonia mydas*), and lamprey (*Petromyzon marinus*). Data are representative of 3-5 independent experiments with n=3-6 replicates per group. Data were analyzed using two-way ANOVA with Šidák's multiple comparisons test. ns = not significant, **** = p<0.0001.

NF-κB activation is a shared function of RHIM-containing proteins and can be tuned by the RHIM

Given that activation of NF-κB by RIPK3 is dependent the RHIM, we hypothesized that the core RHIM tetrad and activation of NF-κB would be broadly conserved across all RHIM-containing proteins, including RIPK1, ZBP1 and TRIF. We found that the RIPK1 RHIM is highly conserved in vertebrates and in RIPK1-like proteins found in zebra mussel, *Linglula* species, and multiple lancelet species (Fig 4A). Human RIPK1 is known to activate NF-κB independently of its RHIM through polyubiquitination of the intermediate domain [32, 33]. However, the strong conservation of the RHIM domain tetrad sequence (V/I-Q-V/I-G) of RIPK1 across species led us to hypothesize that RHIM-mediated activation of NF-κB by RIPK1 is also conserved. We therefore tested a diverse panel of metazoan RIPK1 proteins in our NF-κB assay. To avoid the effects of both kinase activity and kinase-mediated interactions [34], we generated RIPK1 C-terminus ($RIPK1^{CT}$)

280 proteins from diverse species that do (mouse, pig) and do not (cat, lizard, lamprey, zebra
281 mussel) retain all necroptosis proteins (Supplementary Figure 10). Both WT and RHIM
282 mutant human RIPK1^{CT} activate NF-κB to the same extent as full length RIPK1
283 (Supplementary Figure 11), validating our use of this system to characterize RIPK1
284 functions independent from the kinase domain. Diverse vertebrate RIPK1^{CT} proteins
285 activate NF-κB independent of endogenous RIPK1 (Supplementary Figure 12),
286 consistent with our hypothesis that NF-κB activation is an ancestral and conserved
287 function of these proteins. However, like RIPK3, the specific sequence requirements for
288 RIPK1-mediated NF-κB activation varied by species. Specifically, mutation of the RHIM
289 domain does not affect activation of NF-κB by mammalian proteins, including human,
290 mouse, cat, and pig (Figure 4B, left). In contrast, mutation of the RHIM domain attenuated
291 or completely prevented the ability of non-mammalian (lizard, sea lamprey, and zebra
292 mussel) RIPK1^{CT} to activate NF-κB (Figure 4B, right).

293 Other than RIPK1 and RIPK3, only two other human proteins contain a RHIM
294 domain, TRIF and ZBP1. The TRIF RHIM and the first RHIM of ZBP1 are also highly
295 conserved in mammals and some other tetrapods, whereas the second RHIM of ZBP1
296 diverges even within mammals (Fig 4C, Supplementary Figure 13A). We then tested for
297 RHIM-dependence of NF-κB activation by human TRIF and ZBP1. As described
298 previously [35], ZBP1 activates NF-κB in a RHIM- and RIPK1-dependent manner (Fig
299 4D). Consistent with our evolutionary prediction, only the first RHIM tetrad is required for
300 NF-κB activation by ZBP1 (Fig 4D). Conversely, mutation of the TRIF RHIM domain does
301 not affect activation of NF-κB, and activation is only moderately reduced in RIPK1 KO
302 cells (Supplementary Figure 13B-C), likely due to the TIR domain in TRIF that is known
303 to mediate its innate immune signaling [36].

304 Finally, due to the central role of the core tetrad of the RHIM domain, we tested
305 the plasticity of RHIM function with regard to sequence divergence. In our phylogenetic
306 analyses of RIPK3, we identified several species in which the RHIM core tetrad has
307 diverged, particularly outside of tetrapods, including tetrads that have diverged from the
308 conserved motif (V/I-Q-V/I-G) at only a single residue (Supplementary Table 2). To test
309 for functional differences, we inserted these naturally-occurring RHIM tetrads into human

310 RIPK3 and characterized the ability to activate NF-κB and cell death. We included tetrads
311 found in rodents, bats, eulipotyphlans, reptiles, and fish (VQFG), amphibians and fish
312 (LQIG, VQSG), fish (CQIG), and sea lamprey (TQIG). Interestingly, while most tested
313 variants activate NF-κB compared to the inactive RIPK3 RHIM mutant (AAAA tetrad),
314 albeit lower than the WT (VQVG) tetrad, TQIG and VQSG did not activate NF-κB (Fig 4E,
315 Supplementary Figure 14-15). These data suggest that, while there is some plasticity in
316 the RHIM tetrad, not all residues are functional. All tetrad variants were able to activate
317 ZBP1-dependent cell death similar to WT RIPK3 (Fig 4F), further revealing the separation
318 of RIPK3-mediated NF-κB activation from cell death activation. These differences may
319 be due to differential amyloid structures formed during heterooligomerization of the RIPK1
320 RHIM and RIPK3 RHIM versus homooligomerization of RIPK3 [2]. Altogether, these data
321 suggest that diversity in the RIPK3 RHIM domain may tune activation of NF-κB and tailor
322 RIPK3 function to the specific needs of species.

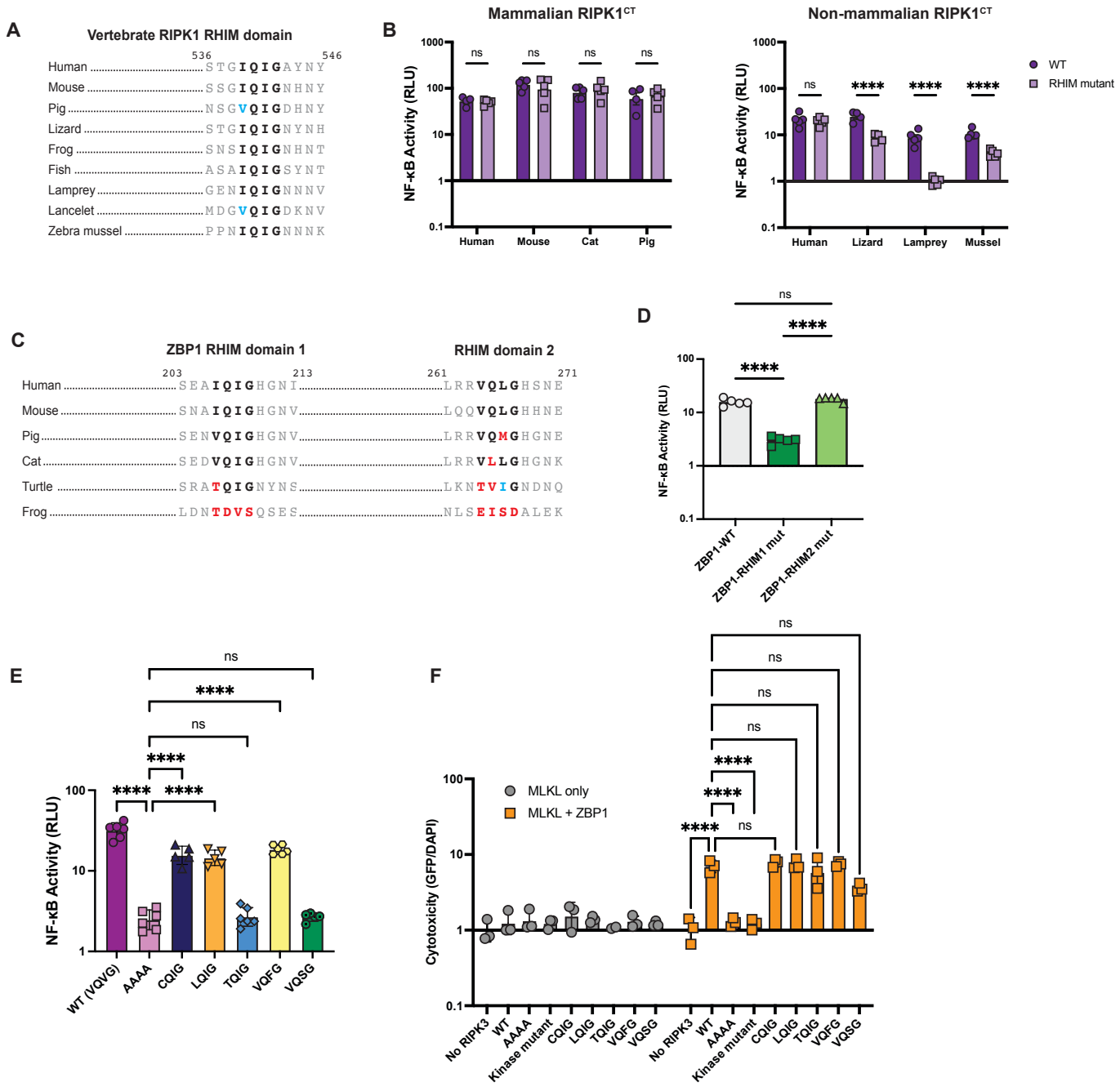

Figure 4. NF-κB activation is a shared function of RHIM-containing proteins and can be tuned by the RHIM. (A) Alignment of RIPK1 RHIM across diverse vertebrates. Residue numbers refer to the human sequence. Lancelet species is *Branchiostoma floridae*. (B) Diverse vertebrate RIPK1^{CT} proteins. were transfected into HEK293T cells along with NF-κB firefly luciferase and control renilla luciferase reporter plasmids (see Materials and Methods), and NF-κB activity was measured at 18h post-transfection. (C) Alignment of ZBP1 RHIMs across diverse vertebrates. Residue numbers refer to the human sequence. (D) Activation of NF-κB by WT and RHIM mutant ZBP1 proteins. (E) NF-κB activation by human RIPK3 with the indicated RHIM tetrad variant. (F) Human RIPK3 proteins with the indicated RHIM tetrad variants were transfected into HEK293T cells with MLKL (gray circles) or MLKL and ZBP1 (orange squares) and viability was measured at 18h post-transfection. Data are representative of 2-5 independent experiments with n=3-6 replicates per group. Data were analyzed using two-way ANOVA

with Šidák's multiple comparisons test (A, D) one-way ANOVA with Tukey's multiple comparisons test (E), or two-way ANOVA with Tukey's multiple comparisons test (F). ns = not significant, **** = p<0.0001.

Discussion

Activation of NF-κB is critical to both the innate and adaptive immune response in humans and mice [20], and is a deeply conserved pathway in many metazoans [24-26]. Despite this deep conservation of NF-κB signaling, differences in the function and regulation of NF-κB-associated proteins between mice and humans have been identified [20], suggesting that this functionally well-conserved pathway can be adapted to different species. These data indicate that broader phylogenetic analysis of the genes and functions that are associated with NF-κB signaling are needed to understand immune responses across species, including those that harbor pathogens that pose a zoonotic threat to humans. Importantly, the approach used here can be applied to other NF-κB-associated proteins, and to other innate immune pathways, to better define species-specific immune responses.

Here, we apply broad phylogenetic and functional sampling to the RIP kinase family of NF-κB activators. Using a phylogenomic approach, we identified widespread conservation of RIPK1, RIPK2, and RIPK4 and their associated proteins within vertebrates. We also show conservation of activation of NF-κB signaling by RIPK1 and RIPK3 across diverse vertebrate species that is largely reliant on the highly conserved core tetrad of the RHIM domains found in both proteins. This striking conservation of RIPK1- and RIPK3-mediated activation of NF-κB, from species that span >500 million years of vertebrate evolution, underscores the core functionality of RIP kinases as NF-κB activating proteins. Despite this conservation of NF-κB activation, we also observed lineage specific changes in RIPK presence or mechanisms of NF-κB activation. For instance, we observed recurrent gene loss of RIPK3 and RIPK5 throughout the vertebrate phylogeny, and discovered a second paralog of RIPK2 in many non-mammalian vertebrate species (RIPK2B). In addition, although RIPK3-mediated activation of NF-κB is highly dependent on RIPK1 across diverse mammals, RIPK3 activation of NF-κB in reptiles is independent of RIPK1. Activation of NF-κB is part of the antiviral immune response and is known to be antagonized by viruses across a range of species, including

367 vertebrates and non-vertebrates [37-39]. This antagonism could result in adaptation of
368 NF-κB-associated proteins, including RIP kinases, leading to lineage-specific
369 mechanisms of activation that are tailored to the specific contexts within and between
370 species.

371 The most striking differences in RIPK-associated genes and functions are those
372 involved in necroptosis. Necroptosis is highly inflammatory and the associated proteins
373 must therefore be tightly regulated, as it could be a cause of immunopathology during
374 infection. Despite this, necroptosis has been shown to be important for the response to
375 several viruses [40-42]. It is hypothesized that necroptosis, defined by RIPK3-mediated
376 activation of MLKL, arose in vertebrates [9, 43]. Interestingly, we find that two critical
377 regulators of necroptosis, CASP8 and ZBP1, are only found in tetrapods, suggestive of
378 an additional innovation within the necroptosis pathway during the divergence of
379 tetrapods. Moreover, consistent with previous observations [9, 10], we observe a large
380 number of necroptosis-associated gene losses, while also discovering important
381 functional motifs in necroptosis proteins in distinct tetrapod lineages. These data support
382 a model where necroptosis has been constructed as an important facet of the innate
383 immune response in some tetrapods, but is not universal and has been deconstructed in
384 species where the immunopathologic effects outweigh the benefits.

385 There have been several hypotheses to explain the loss of necroptosis associated
386 proteins in specific vertebrate lineages, such as diet (*e.g.,* carnivores) or behavior (*e.g.,*
387 torpor in reptiles) [9]. While the cause of a specific instance of gene loss is difficult to
388 identify, it is clear that gene loss can provide an evolutionary tool for adaptation [44].For
389 example, caspases, which are key regulators of both immunologically silent apoptosis
390 and inflammatory pyroptosis, differ greatly across mammals, with lineage-specific
391 caspase repertoires including both loss and gain of novel caspases [28]. Even within a
392 single mammalian order, homologous caspases have been found to serve different
393 functions in response to pathogens [45]. This type of lineage-specific innovation likely
394 exists for necroptosis, and gene loss could be a cause or a result of adaptations. Indeed,
395 differences in MLKL activation by RIPK3 across species have been identified [46], which
396 may be the result of additional diverse regulatory mechanisms for necroptosis even
397 amongst species with an intact pathway. Strikingly, despite the lack of a complete

398 necroptosis pathway in some lineages (cat, turtle, lamprey), our functional data indicate
399 that RIPK3 retains the ability to activate NF-κB. Activation of NF-κB could therefore
400 represent the ancestral function of RIPK3, and it has been co-opted to activate
401 necroptosis in vertebrates.

402 The RHIM core tetrad was previously known to be conserved between humans and
403 mice [47]. Here, we expand this analysis and identify striking conservation of the RIPK3,
404 RIPK1, ZBP1, and TRIF RHIM domains across most vertebrates. Additional RHIM-
405 containing proteins have been identified in non-vertebrate animals and in fungi [48].
406 Interestingly, the RHIM proteins found in fruit fly and fungi are known to be involved in
407 antibacterial defense and cell death, respectively, suggesting that RHIM-mediated
408 interactions may be an ancient mechanism of innate immunity. While activation of NF-κB
409 by all tested non-human RIPK3 proteins was highly dependent on the RHIM domain, only
410 non-mammalian RIPK1^{CT} proteins required the RHIM for maximal NF-κB activation.
411 These species (lizard, lamprey, and zebra mussel) also lack ZBP1, with lamprey and
412 zebra mussel predating the emergence of ZBP1 in tetrapods. Necroptosis may have
413 driven evolution of RHIM-independent activation of NF-κB by RIPK1. This may have also
414 shaped RHIM-dependent functions of RIPK3 across vertebrates, as the RHIM tetrad is
415 much less conserved in fish compared to tetrapods, and insertion of these tetrad variants
416 into human RIPK3 alters its function. Virus antagonism has also likely played a role in the
417 evolution of RIPK3 and RIPK1 function. For example, vaccinia virus E3 prevents Z-DNA
418 sensing by ZBP1 [40], human cytomegalovirus UL36 promotes MLKL degradation, and
419 poxviruses encode an MLKL homolog to prevent RIPK3-mediated activation of host MLKL
420 [49]. Conservation of the RHIM domain may be a way to retain some RIPK3/RIPK1 innate
421 immune functions in the face of such antagonism. However, several viruses have taken
422 advantage of this conservation and encode RHIM-containing proteins to prevent RHIM-
423 dependent functions [43, 47]. Intriguingly, several of these mechanisms are known to be
424 species-specific and differ between humans and mice [14, 15]. These data support a
425 model where viruses and host necroptosis are engaged in a molecular arms race that has
426 shaped the function of RIPK3 and RIPK1 across vertebrate species.

427 Altogether, our combined phylogenetic and functional approaches reveal both
428 conservation and a striking lack of conservation in vertebrate RIPKs and their associated

429 proteins and functions. Such characteristics are common hallmarks of pathways that are
430 required for the innate immune response to pathogens, but are under constant
431 evolutionary pressure to innovate to avoid pathogen antagonism. The strong conservation
432 of NF-κB activation by RIPK1 across species is consistent with the model in which RIPK1
433 function is central to determining cell fate downstream of TNF and TLR signaling [50].
434 Moreover, because some pathogens have evolved strategies to inhibit CASP8, RIPK3-
435 and RIPK1-mediated necroptosis is activated as a secondary cell death strategy when
436 CASP8 is inhibited [51]. This places both RIPK3 and RIPK1, critical regulators of
437 necroptosis, at the center of determining cell fate during pathogen infection. The
438 divergence of RIPK3 and RIPK1 across vertebrates identified here, as well as the
439 previous finding that these proteins are evolving under positive selection [10, 17, 18],
440 reveals that pathogens are likely the driving force behind the lineage-specific regulatory
441 mechanisms or functions of these proteins across species that we observe here. Thus,
442 the functional divergence identified in our work highlights the evolutionary innovation that
443 can arise in innate signaling pathways across diverse species, and underscores the
444 importance of considering natural diversity when characterizing the innate immune
445 response to pathogens. Our work provides a model for further study on the diversity of
446 innate immune proteins, protein families, and pathways across vertebrate and non-
447 vertebrate species.
448

449 **Materials & Methods**

450 *Positive selection analysis*

451 Positive selection analysis was performed using three independent methods as we
452 have done previously [52, 53]. Nucleotide sequences from the indicated mammalian
453 clade that aligned to full-length human RIPK1-5 were downloaded from NCBI and aligned
454 using ClustalOmega [54]. Maximum likelihood (ML) tests were performed with codeml in
455 the PAML software suite [55]. For PAML, aligned sequences were subjected to ML tests
456 using NS sites models disallowing (M7) or allowing (M8) positive selection. The reported
457 p-values were calculated using a chi-squared test on twice the difference of the log
458 likelihood (lnL) values between the two models using 2 degrees of freedom. We confirmed
459 convergence of lnL values by performing each analysis using two starting omega (dN/dS)

460 values (0.4 and 1.5). Codons evolving under positive selection from PAML analyses have
461 a posterior probability greater than 0.90 using Native Empirical Bayes (NEB) and Bayes
462 Empirical Bayes (BEB) analysis and the F61 codon frequency model. The same
463 nucleotide alignments were used as input for FUBAR (Fast, Unconstrained Bayesian
464 AppRoximation) [56] and MEME (Mixed Effects Model of Evolution) [57] using the
465 DataMonkey server [58]. In both cases, default parameters were used and codons with a
466 signature of positive selection with a p-value of <0.01 are reported. Accession numbers
467 for input sequences, PAML p-values, and sites identified can be found in Supplementary
468 Files 1-3.
469
470 *Gene loss analysis*
471 Gene loss analysis was completed by first building phylogenetic trees for each
472 protein of interest. Phylogenetic trees were generated for RIPK1-5 using previously
473 described methods [59]. Briefly, the kinase domains from human RIPK1
474 (NP_001341859.1), RIPK2 (NP_003812.1), RIPK3 (NP_006862.2), RIPK4
475 (NP_065690.2), and RIPK5 (NP_848605.1) were used to query the RefSeq protein
476 database using BLASTp with an e-value cutoff of 2e-26 [60]. While LRRK1 and LRRK2
477 share kinase homology with RIPK1-5 and are sometimes known as RIPK6 and -7 [23],
478 they have a distinct domain structure and function compared to RIPK1-5 and will therefore
479 not be considered as RIP kinases for the purposes of this study. The five resulting
480 sequence lists were consolidated to a single list of unique sequences using Geneious
481 software. These sequences were then aligned using Clustal Omega [54] with two
482 refinement iterations implemented in Geneious software. Following alignment, we filtered
483 sequences based on alignment of an N-terminal kinase domain to human RIPK kinase
484 domains and the presence of a C-terminal domain. Proteins with additional N-terminal
485 domains, proteins lacking homology to human kinase domains, and proteins lacking C-
486 terminal domains were removed. Using the aligned and filtered vertebrate RIPK
487 sequences (4,550 sequences in total), a tree was built using FastTree [61, 62]
488 implemented using Geneious. Vertebrate MAPKK7 sequences were used as an outgroup
489 to help isolate RIP kinases from similar, but distinct, kinases. Using this tree, we were
490 able to identify and extract *bona fide* RIP kinases. The extracted sequences were again

491 aligned using Clustal Omega and filtered using the criteria above. A second tree was
492 generated using FastTree. From this tree, we extracted individual sequence lists for
493 RIPK1-5 to determine which vertebrate species did or did not have each RIPK. This
494 method was repeated for, MLKL, TRIF, FADD, CASP8 and 10, NOD 1 and 2, and IRF6.
495 The list of species and lists of accession numbers for each protein can be found in
496 Supplementary Files 4 and 5. A list of outgroups used for each analyzed protein can be
497 found in Supplementary File 6.
498
499 *Plasmids and constructs*
500 Coding sequences for human RIPK1 (Addgene #78834), human RIPK2
501 (ORFeome ID #4886), human RIPK3 (Addgene #78804), mouse RIPK1 (Addgene
502 #115341), and mouse RIPK3 (Addgene #78805) were cloned into apcDNA5/FRT/TO
503 backbone (Invitrogen, Carlsbad, CA) with an N-terminal V5 tag and linker using Gibson
504 Assembly (New England Biolabs, Ipswich, MA). Human RIPK4 (NP_065690.2) and
505 RIPK5 (NP_848605.1), and non-human RIPK1 C-termini (cat, XP_023109490.2; pig,
506 XP_003128209.1; chicken, NP_989733.3; lizard, XP_003224434.1; lamprey,
507 XP_032813622.1; zebra mussel, XP_052232845.1) and RIPK3 (cat, XP_003987615.3;
508 pig, XP_001927459.3; lizard, XP_003223896.2; turtle, XP_037771912.1; lamprey,
509 XP_032816533.1) homologues were ordered from Twist Biosciences (San Francisco,
510 CA, USA) and were cloned along with RHIM mutants targeting the core tetrad into the
511 pcDNA5/FRT/TO backbone (Invitrogen, Carlsbad, CA) with an N-terminal V5 tag and
512 linker using Gibson Assembly (New England Biolabs, Ipswich, MA). Kinase mutants for
513 human proteins RIPK1 (D138N), RIPK2 (D146N), RIPK3 (D142N), RIPK4 (D143N), and
514 RIPK5 (D145N), and RHIM mutants for RIPK1 (IQIG542AAAA) and RIPK3
515 (VQVG461AAAA) were generated using Gibson Assembly.
516
517 *Cell culture and transient transfections*
518 HEK293T cells (obtained from ATCC) and the generated HEK293T RIPK1 KO cells
519 were maintained at a low passage number to maintain less than one year since
520 purchase, acquisition, or generation. Both cell lines were grown in complete media
521 containing DMEM (Gibco, Carlsbad, CA), 10% FBS (Peak Serum, Wellington, CO), and

522 1% penicillin/streptomycin (Gibco, Carlsbad, CA). A day prior to transfection, HEK293T
523 and RIPK1 KO cells were seeded into 24-well plates with 500 µL complete media or 96-
524 well plates with 80 µL complete media. Cells were transiently transfected with 500 ng
525 total DNA and 1.5 µL of TransIT-X2 (Mirus Bio, Madison, WI) in 100 µL Opti-MEM
526 (Gibco, Carlsbad, CA) for a 24-well plate or 100 ng DNA and 0.3 µL TransIT-X2 in 10
527 µL Opti-MEM for a 96-well plate. DNA and TransIT-X2 were incubated at room
528 temperature for 25-30 minutes, then added dropwise to the appropriate well. Cells were
529 harvested or analyzed at 18-22 hours post-transfection.
530
531 *Generation of knockout cell lines*
532 RIPK1 knockout HEK293T cells were generated using CRISPR/Cas9 as
533 previously described [53, 63]. Briefly, plasmids were generated order to produce
534 lentivirus-like particles containing the CRISPR/Cas9 machinery and guide RNA targeting
535 exon 5 (ENSE00003586162) of RIPK1. The protocol for the molecular cloning of this
536 plasmid was adapted from Feng Zhang (Sanjana et al., 2014) using the transfer plasmid
537 pLB-Cas9 (gift from Feng Zhang, Addgene plasmid # 52962). We designed the gRNA
538 target sequence using the web tool CHOPCHOP (Labun et al., 2016), available at
539 https://chopchop.cbu.uib.no/, and synthesized oligonucleotides from Integrated DNA
540 Technologies (San Diego, CA). The synthesized oligonucleotide pair was phosphorylated
541 and annealed using T4 Polynucleotide Kinase (NEB M0201S) with T4 Ligation Buffer
542 (NEB). Duplexed oligonucleotides were ligated into dephosphorylated and BsmBI-
543 digested pLB-Cas9 using the Quick Ligase kit (NEB M2200S) to generate transfer
544 plasmid with RIPK1 guide sequence. To generate lentivirus-like particles, this transfer
545 plasmid was transfected alongside two packaging plasmids, pMD2.G (gift from Didier
546 Trono, Addgene plasmid # 12259) and psPAX2 (gift from Didier Trono, Addgene plasmid
547 # 12260), into HEK293T cells with a 1:1:1 stoichiometry. Forty-eight hours post-
548 transfection supernatant was harvested and syringe-filtered (0.45µm). Supernatant
549 containing sgRNA-encoding lentivirus-like particles was then used to transduce HEK293T
550 cells. Transduced cells were cultured in growth media for 48 hours, then cultured in
551 growth media supplemented with 1 µg/ml puromycin for 72 hours. Using limiting dilution

552 in 96-well plates, the monoclonal cell line was then obtained. RIPK1 knockout was
553 confirmed by Sanger sequencing and by western blot using an α-RIPK1 antibody.
554
555 *NF-κB and IFN luciferase reporter assays*
556 To quantify NF-κB and IFN activation, we used the Dual-Glo Luciferase Assay
557 System E2920 (Promega, USA). WT or RIPK1 KO HEK293T cells were seeded in a white
558 96-well plate and transfected with firefly luciferase fused to either the NF-κB response
559 element (pGL4.32, Promega) or the human IFN-beta promoter (IFN-Beta-pGL3, Addgene
560 #102597), renilla luciferase fused to herpes simplex virus thymidine kinase promoter
561 (pTK-Renilla, Thermo Scientific), and the indicated RIPK. Firefly luciferase was used as
562 the primary reporter with renilla luciferase being a normalization control. Eighteen to 24
563 hours after transfection, Dual-Glo Luciferase Assay Reagent was added to each
564 transfected well as well as 3-6 untransfected wells to serve as a negative control.
565 Following a 10-minute incubation, the firefly luciferase signal was measured using a
566 BioTek Cytation imaging reader with Gen5 software (Agilent Technologies, San Diego,
567 CA). Then, Dual-Glo Stop & Glo reagent was added to each well. Following a 10-minute
568 incubation, the renilla luciferase signal was measured. The background luminescence
569 signal from the buffer-treated untransfected conditions was subtracted from other
570 conditions, firefly values were normalized to renilla values, and all samples were
571 normalized to the empty vector control condition. Values are reported as NF-κB activity
572 (firefly/renilla).
573
574 *Cell death assay*
575 Cell viability was measured using the ReadyProbes Cell Viability Imaging Kit, Blue/Green
576 (ThermoFisher Scientific). HEK293T cells were seeded in 80 µL of DMEM+/+ (See "Cell
577 culture and transient transfections") in a clear 96-well plate and transfected with the
578 indicated plasmids or a vector control. Eighteen hours post-transfection, cells were
579 stained using NucBlue Live reagent, which stains all nuclei, and NucGreen Dead reagent,
580 which stains only dead cells. A 2x concentrated mix (4 drops/mL of each dye) was made
581 and added to wells to 1x concentration. Cells were incubated for 20 minutes at room
582 temperature. Fluorescence for NucBlue (DAPI, excitation 377/20, emission 447/20) and

583 NucGreen (GFP, excitation 469/20, emission 525/20) were read using a BioTek Cytation
584 imaging reader with Gen5 software (Agilent Technologies, San Diego, CA). Unstained
585 wells were read and used as controls for background fluorescence. GFP values were
586 normalized to DAPI values, and all samples were normalized to the vector control
587 condition. Values are reported as Cytotoxicity (GFP/DAPI).
588
589 *Immunoblotting and antibodies*
590 Eighteen to 22 hours post-transfection, cells were washed with 1X PBS and lysed with
591 boiling 1x NuPAGE LDS sample buffer containing 5% β-mercaptoethanol at room
592 temperature for 5 minutes and then at 98°C for 7-10 minutes. Lysates were separated
593 by SDS-PAGE (4-15% Bis-tris gel; Life Technologies, San Diego, CA) with 1X MOPS
594 buffer (Life Technologies, San Diego, CA). Proteins were transferred onto a
595 nitrocellulose membrane (Life Technologies, San Diego, CA) and blocked with PBS–T
596 containing 5% bovine serum albumin (BSA) (Spectrum, New Brunswick, NJ).
597 Membranes were incubated with the indicated rabbit primary antibodies diluted with 5%
598 BSA and PBS-T at 1:1000 overnight at 4°C (α-V5 clone D3H8Q, α-GAPDH clone
599 14C10, α-RIPK1 clone E8S7U XP, α-RIPK2 clone D10B11, α-RIPK3 clone E1Z1D, α-
600 RIPK4 #12636; Cell Signaling Technology, Danvers, MA). Membranes were rinsed
601 three times with PBS-T, incubated with HRP-conjugated rabbit secondary antibody
602 diluted at 1:10,000 with 5% BSA and PBS-T for 30 minutes at room temperature, and
603 developed with SuperSignal West Pico PLUS Chemiluminescent Substrate (Thermo
604 Fisher Scientific, Carlsbad, CA).
605
606 *Statistical analysis*
607 Statistical analyses were completed using GraphPad Prism 10 software. Tests were
608 performed as indicated. Error bars were calculated using SEM.
609
610 **Acknowledgements**
611 This work was supported by National Institutes of Health grant R35 GM133633 (to MDD); Pew
612 Biomedical Scholars Program (to MDD); Burroughs Wellcome Investigators in the Pathogenesis
613 of Infectious Disease Program (to MDD); and BrightSpinnaker Fellowship (to CMR). We thank all

members of the Daugherty lab for helpful discussions and Scott Biering, Ryan Langlois, and Patrick Mitchell for their critical reading of this manuscript.

Conflict of Interest

The authors declare that they have no conflict of interest.

References

1. Newton, K., *RIPK1 and RIPK3: critical regulators of inflammation and cell death.* Trends Cell Biol, 2015. **25**(6): p. 347-53.
2. Wu, X., et al., *The structure of a minimum amyloid fibril core formed by necroptosis-mediating RHIM of human RIPK3.* Proc Natl Acad Sci U S A, 2021. **118**(14).
3. Sun, L., et al., *Mixed lineage kinase domain-like protein mediates necrosis signaling downstream of RIP3 kinase.* Cell, 2012. **148**(1-2): p. 213-27.
4. Wang, L., F. Du, and X. Wang, *TNF-alpha induces two distinct caspase-8 activation pathways.* Cell, 2008. **133**(4): p. 693-703.
5. Mandal, P., et al., *RIP3 induces apoptosis independent of pronecrotic kinase activity.* Mol Cell, 2014. **56**(4): p. 481-95.
6. Meylan, E., et al., *RIP1 is an essential mediator of Toll-like receptor 3-induced NF-kappa B activation.* Nat Immunol, 2004. **5**(5): p. 503-7.
7. Moriwaki, K., et al., *The necroptosis adaptor RIPK3 promotes injury-induced cytokine expression and tissue repair.* Immunity, 2014. **41**(4): p. 567-78.
8. Orozco, S. and A. Oberst, *RIPK3 in cell death and inflammation: the good, the bad, and the ugly.* Immunol Rev, 2017. **277**(1): p. 102-112.
9. Dondelinger, Y., et al., *An evolutionary perspective on the necroptotic pathway.* Trends Cell Biol, 2016. **26**(10): p. 721-732.
10. Agueda-Pinto, A., et al., *Convergent Loss of the Necroptosis Pathway in Disparate Mammalian Lineages Shapes Viruses Countermeasures.* Front Immunol, 2021. **12**: p. 747737.
11. Harris, K.G., et al., *RIP3 Regulates Autophagy and Promotes Coxsackievirus B3 Infection of Intestinal Epithelial Cells.* Cell Host Microbe, 2015. **18**(2): p. 221-32.
12. Croft, S.N., E.J. Walker, and R. Ghildyal, *Human Rhinovirus 3C protease cleaves RIPK1, concurrent with caspase 8 activation.* Sci Rep, 2018. **8**(1): p. 1569.
13. Wagner, R.N., J.C. Reed, and S.K. Chanda, *HIV-1 protease cleaves the serine-threonine kinases RIPK1 and RIPK2.* Retrovirology, 2015. **12**: p. 74.
14. Muscolino, E., et al., *Species-Specific Inhibition of Necroptosis by HCMV UL36.* Viruses, 2021. **13**(11).
15. Huang, Z., et al., *RIP1/RIP3 binding to HSV-1 ICP6 initiates necroptosis to restrict virus propagation in mice.* Cell Host Microbe, 2015. **17**(2): p. 229-42.
16. Liu, X., et al., *Epstein-Barr virus encoded latent membrane protein 1 suppresses necroptosis through targeting RIPK1/3 ubiquitination.* Cell Death Dis, 2018. **9**(2): p. 53.

656 17. Palmer, S., et al., *Evolutionary profile for (host and viral) MLKL indicates its*
657 *activities as a battlefront for extensive counteradaptation.* Mol Biol Evol, 2021.
658 **38**(12): p. 5405-522.
659 18. Cariou, M., et al., *Distinct evolutionary trajectories of SARS-CoV-2-interacting*
660 *proteins in bats and primates identify important host determinants of COVID-19.*
661 Proc Natl Acad Sci U S A, 2022. **119**(35): p. e2206610119.
662 19. Daugherty, M.D. and H.S. Malik, *Rules of engagement: molecular insights from*
663 *host-virus arms races.* Annu Rev Genet, 2012. **46**: p. 677-700.
664 20. Zhang, Q., M.J. Lenardo, and D. Baltimore, *30 Years of NF-kappaB: A Blossoming*
665 *of Relevance to Human Pathobiology.* Cell, 2017. **168**(1-2): p. 37-57.
666 21. Cuny, G.D. and A. Degterev, *RIPK protein kinase family: Atypical lives of typical*
667 *kinases.* Semin Cell Dev Biol, 2021. **109**: p. 96-105.
668 22. Eng, V.V., M.A. Wemyss, and J.S. Pearson, *The diverse roles of RIP kinases in*
669 *host-pathogen interactions.* Semin Cell Dev Biol, 2021. **109**: p. 125-143.
670 23. Lv, S., et al., *Comparative and evolutionary analysis of RIP kinases in immune*
671 *responses.* Front Genet, 2022. **13**: p. 796291.
672 24. Wang, X.W., et al., *Evidence for the ancient origin of the NF-kappaB/IkappaB*
673 *cascade: its archaic role in pathogen infection and immunity.* Proc Natl Acad Sci U
674 S A, 2006. **103**(11): p. 4204-9.
675 25. Hetru, C. and J.A. Hoffmann, *NF-kappaB in the immune response of Drosophila.*
676 Cold Spring Harb Perspect Biol, 2009. **1**(6): p. a000232.
677 26. Williams, L.M. and T.D. Gilmore, *Looking Down on NF-kappaB.* Mol Cell Biol,
678 2020. **40**(15).
679 27. Rodriguez, D.A., et al., *Caspase-8 and FADD prevent spontaneous ZBP1*
680 *expression and necroptosis.* Proc Natl Acad Sci U S A, 2022. **119**(41): p.
681 e2207240119.
682 28. Eckhart, L., et al., *Identification of novel mammalian caspases reveals an important*
683 *role of gene loss in shaping the human caspase repertoire.* Mol Biol Evol, 2008.
684 **25**(5): p. 831-41.
685 29. Yatim, N., et al., *RIPK1 and NF-kappaB signaling in dying cells determines cross-*
686 *priming of CD8(+) T cells.* Science, 2015. **350**(6258): p. 328-34.
687 30. Benton, M.J. and P.C. Donoghue, *Paleontological evidence to date the tree of life.*
688 Mol Biol Evol, 2007. **24**(1): p. 26-53.
689 31. Sun, X., et al., *Identification of a novel homotypic interaction motif required for the*
690 *phosphorylation of receptor-interacting protein (RIP) by RIP3.* J Biol Chem, 2002.
691 **277**(11): p. 9505-11.
692 32. Li, H., et al., *Ubiquitination of RIP is required for tumor necrosis factor alpha-*
693 *induced NF-kappaB activation.* J Biol Chem, 2006. **281**(19): p. 13636-13643.
694 33. Ea, C.K., et al., *Activation of IKK by TNFalpha requires site-specific ubiquitination*
695 *of RIP1 and polyubiquitin binding by NEMO.* Mol Cell, 2006. **22**(2): p. 245-57.
696 34. Delanghe, T., Y. Dondelinger, and M.J.M. Bertrand, *RIPK1 Kinase-Dependent*
697 *Death: A Symphony of Phosphorylation Events.* Trends Cell Biol, 2020. **30**(3): p.
698 189-200.
699 35. Rebsamen, M., et al., *DAI/ZBP1 recruits RIP1 and RIP3 through RIP homotypic*
700 *interaction motifs to activate NF-kappaB.* EMBO Rep, 2009. **10**(8): p. 916-22.

701 36. Nanson, J.D., B. Kobe, and T. Ve, *Death, TIR, and RHIM: Self-assembling*
702 *domains involved in innate immunity and cell-death signaling.* J Leukoc Biol, 2019.
703 **105**(2): p. 363-375.
704 37. Albarnaz, J.D., et al., *Molecular mimicry of NF-kappaB by vaccinia virus protein*
705 *enables selective inhibition of antiviral responses.* Nat Microbiol, 2022. **7**(1): p.
706 154-168.
707 38. Gonzalez Lopez Ledesma, M.M., et al., *Dengue virus NS5 degrades ERC1 during*
708 *infection to antagonize NF-kB activation.* Proc Natl Acad Sci U S A, 2023. **120**(23):
709 p. e2220005120.
710 39. Palmer, W.H., et al., *Induction and Suppression of NF-kappaB Signalling by a DNA*
711 *Virus of Drosophila.* J Virol, 2019. **93**(3).
712 40. Koehler, H., et al., *Vaccinia virus E3 prevents sensing of Z-RNA to block ZBP1-*
713 *dependent necroptosis.* Cell Host Microbe, 2021. **29**(8): p. 1266-1276 e5.
714 41. Balachandran, S. and G.F. Rall, *Benefits and Perils of Necroptosis in Influenza*
715 *Virus Infection.* J Virol, 2020. **94**(9).
716 42. Shubina, M., et al., *Necroptosis restricts influenza A virus as a stand-alone cell*
717 *death mechanism.* J Exp Med, 2020. **217**(11).
718 43. Tummers, B. and D.R. Green, *The evolution of regulated cell death pathways in*
719 *animals and their evasion by pathogens.* Physiol Rev, 2022. **102**(1): p. 411-454.
720 44. Albalat, R. and C. Canestro, *Evolution by gene loss.* Nat Rev Genet, 2016. **17**(7):
721 p. 379-91.
722 45. Devant, P., A. Cao, and J.C. Kagan, *Evolution-inspired redesign of the LPS*
723 *receptor caspase-4 into an interleukin-1beta converting enzyme.* Sci Immunol,
724 2021. **6**(62).
725 46. Tanzer, M.C., et al., *Evolutionary divergence of the necroptosis effector MLKL.* Cell
726 Death Differ, 2016. **23**(7): p. 1185-97.
727 47. Riebeling, T., U. Kunzendorf, and S. Krautwald, *The role of RHIM in necroptosis.*
728 Biochem Soc Trans, 2022. **50**(4): p. 1197-1205.
729 48. Kajava, A.V., et al., *Evolutionary link between metazoan RHIM motif and prion-*
730 *forming domain of fungal heterokaryon incompatibility factor HET-s/HET-s.* Sci
731 Rep, 2014. **4**: p. 7436.
732 49. Petrie, E.J., et al., *Viral MLKL Homologs Subvert Necroptotic Cell Death by*
733 *Sequestering Cellular RIPK3.* Cell Rep, 2019. **28**(13): p. 3309-3319 e5.
734 50. Clucas, J. and P. Meier, *Roles of RIPK1 as a stress sentinel coordinating cell*
735 *survival and immunogenic cell death.* Nat Rev Mol Cell Biol, 2023. **24**(11): p. 835-
736 852.
737 51. Remick, B.C., M.M. Gaidt, and R.E. Vance, *Effector-Triggered Immunity.* Annu
738 Rev Immunol, 2023. **41**: p. 453-481.
739 52. Tsu, B.V., et al., *Host-specific sensing of coronaviruses and picornaviruses by the*
740 *CARD8 inflammasome.* PLoS Biol, 2023. **21**(6): p. e3002144.
741 53. Stevens, D.A., et al., *Antiviral function and viral antagonism of the rapidly evolving*
742 *dynein activating adaptor NINL.* Elife, 2022. **11**.
743 54. Sievers, F., et al., *Fast, scalable generation of high-quality protein multiple*
744 *sequence alignments using Clustal Omega.* Mol Syst Biol, 2011. **7**: p. 539.
745 55. Yang, Z., *PAML 4: phylogenetic analysis by maximum likelihood.* Mol Biol Evol,
746 2007. **24**(8): p. 1586-91.

747 56. Murrell, B., et al., *FUBAR: a fast, unconstrained bayesian approximation for*
748 *inferring selection.* Mol Biol Evol, 2013. **30**(5): p. 1196-205.
749 57. Murrell, B., et al., *Detecting individual sites subject to episodic diversifying*
750 *selection.* PLoS Genet, 2012. **8**(7): p. e1002764.
751 58. Weaver, S., et al., *Datamonkey 2.0: A Modern Web Application for Characterizing*
752 *Selective and Other Evolutionary Processes.* Mol Biol Evol, 2018. **35**(3): p. 773-
753 777.
754 59. Fu, L., et al., *CD-HIT: accelerated for clustering the next-generation sequencing*
755 *data.* Bioinformatics, 2012. **28**(23): p. 3150-2.
756 60. Altschul, S.F., et al., *Gapped BLAST and PSI-BLAST: a new generation of protein*
757 *database search programs.* Nucleic Acids Res, 1997. **25**(17): p. 3389-402.
758 61. Price, M.N., P.S. Dehal, and A.P. Arkin, *FastTree: computing large minimum*
759 *evolution trees with profiles instead of a distance matrix.* Mol Biol Evol, 2009. **26**(7):
760 p. 1641-50.
761 62. Price, M.N., P.S. Dehal, and A.P. Arkin, *FastTree 2--approximately maximum-*
762 *likelihood trees for large alignments.* PLoS One, 2010. **5**(3): p. e9490.
763 63. Tsu, B.V., et al., *Diverse viral proteases activate the NLRP1 inflammasome.* Elife,
764 2021. **10**.
765